Development 126, 2771-2783 (1999)
Printed in Great Britain © The Company of Biologists Limited 1999
DEV2402

Distinct signaling molecules control *Hoxa-11* and *Hoxa-13* expression in the muscle precursor and mesenchyme of the chick limb bud

Kazue Hashimoto[1], Yuji Yokouchi[1], Masakazu Yamamoto[1,2] and Atsushi Kuroiwa[1,*]

[1]Division of Biological Science, Graduate School of Science, Nagoya University, Furo-cho, Chikusa-ku, Nagoya 464-8602, Japan
[2]CREST, Japan Science and Technology Corporation (JST)
*Author for correspondence (e-mail: i45240a@nucc.cc.nagoya-u.ac.jp)

Accepted 30 March; published on WWW 19 May 1999

SUMMARY

The limb muscles, originating from the ventrolateral portion of the somites, exhibit position-specific morphological development through successive splitting and growth/differentiation of the muscle masses in a region-specific manner by interacting with the limb mesenchyme and the cartilage elements. The molecular mechanisms that provide positional cues to the muscle precursors are still unknown. We have shown that the expression patterns of *Hoxa-11* and *Hoxa-13* are correlated with muscle patterning of the limb bud (Yamamoto et al., 1998) and demonstrated that muscular *Hox* genes are activated by signals from the limb mesenchyme. We dissected the regulatory mechanisms directing the unique expression patterns of *Hoxa-11* and *Hoxa-13* during limb muscle development. HOXA-11 protein was detected in both the myogenic cells and the zeugopodal mesenchymal cells of the limb bud. The earlier expression of HOXA-11 in both the myogenic precursor cells and the mesenchyme was dependent on the apical ectodermal ridge (AER), but later expression was independent of the AER. HOXA-11 expression in both myogenic precursor cells and mesenchyme was induced by fibroblast growth factor (FGF) signal, whereas hepatocyte growth factor/scatter factor (HGF/SF) maintained HOXA-11 expression in the myogenic precursor cells, but not in the mesenchyme. The distribution of HOXA-13 protein expression in the muscle masses was restricted to the posterior region. We found that HOXA-13 expression in the autopodal mesenchyme was dependent on the AER but not on the polarizing region, whereas expression of HOXA-13 in the posterior muscle masses was dependent on the polarizing region but not on the AER. Administration of BMP-2 at the anterior margin of the limb bud induced ectopic HOXA-13 expression in the anterior region of the muscle masses followed by ectopic muscle formation close to the source of exogenous BMP-2. In addition, NOGGIN/CHORDIN, antagonists of BMP-2 and BMP-4, downregulated the expression of HOXA-13 in the posterior region of the muscle masses and inhibited posterior muscle development. These results suggested that HOXA-13 expression in the posterior muscle masses is activated by the posteriorizing signal from the posterior mesenchyme via BMP-2. On the contrary, the expression of HOXA-13 in the autopodal mesenchyme was affected by neither BMP-2 nor NOGGIN/CHORDIN. Thus, mesenchymal HOXA-13 expression was independent of BMP-2 from polarizing region, but was under the control of as yet unidentified signals from the AER. These results showed that expression of *Hox* genes is regulated differently in the limb muscle precursor and mesenchymal cells.

Key words: *Hoxa-11*, *Hoxa-13*, FGF, HGF/SF, BMP-2, Noggin, Chordin, Muscle, Limb bud, Chick

INTRODUCTION

The muscles of the limb develop from the myogenic cells that are derived from the lateral dermamyotome of the somites adjacent to the limb bud (Chevallier et al., 1977). Beginning at stage 15, somitic myogenic precursors migrate into the wing bud due to the interaction between the dermamyotome and the presumptive limb mesenchyme (Hayashi and Ozawa, 1995), and then congregate to form the dorsal muscle masses (DMM) and ventral muscle masses (VMM) (Schramm and Solursh, 1990). The limb muscle pattern develops by sequential splitting of each muscle mass in a region-specific manner, generating individual muscles with characteristic size and shape in appropriate locations (Shellswell and Wolpert, 1977; Robson et al., 1994).

The following factors are known to be involved in the myogenic developmental program. In the initial step, *Pax-3*, which is expressed from the very early stage of paraxial mesoderm formation, controls expression of *c-met* encoding the HGF/SF receptor and transcription factor *lbx1* (Daston et al., 1996; Yang et al., 1996; Mennerich et al., 1998). In the second step, HGF/SF, secreted from the limb mesenchyme, controls delamination of the myogenic precursor cells from the dermamyotomal epithelium and migration of the myogenic precursor cells into the limb buds via c-Met (reviewed in Birchmeier and Gherardi, 1998). A third step is

defined by the effects mediated by the *MyoD* gene family that regulate myogenic cell differentiation (Olson and Klein, 1994). The last step, which includes pattern formation of the limb muscles, is less well understood. Manipulation of the chick wing buds revealed that the limb mesenchyme provides positional cues for limb muscle patterning. For example, when the polarizing region was implanted into the anterior margin of the limb bud, the cartilage, muscles and tendons manifested mirror-image transformation along the anteroposterior axis (Shellswell and Wolpert, 1977; Robson et al., 1994). With regard to the dorsoventral axis, *Wnt7a* in the dorsal ectoderm induced *Lmx1* expression in the dorsal mesenchymal cells. Forced expression of *Lmx1* in the ventral mesenchyme resulted in transformation of the ventral muscles and tendons to the dorsal pattern (Riddle et al., 1995; Vogel et al., 1995). In addition, disruption of the *Wnt7a* gene in mice caused ventralization of the dorsal muscles (Parr and McMahon, 1995). Recent studies showed that SHH and BMPs are crucial for controlling the timing of proliferation and differentiation of the myogenic cells that may be involved in the limb muscle patterning (Duprez et al., 1998; Amthor et al., 1998).

During limb development, *Hox* genes in the *Abdominal-B* (*Abd-B*) subfamily of the *HoxD* and *HoxA* gene cluster are expressed in the limb mesenchyme in a spatially and temporally collinear manner along the anteroposterior and proximodistal axes, respectively (Dolle et al., 1989; Izpisua-Belmonte et al., 1991; Nohno et al., 1991; Yokouchi et al., 1991). Loss-of-function and gain-of-function experiments demonstrated that the *Hox* genes regulate proliferation, differentiation and adhesion of the limb mesenchyme to form cartilage with region-specific morphology (Morgan et al., 1992; Dolle et al., 1993; Small and Potter 1993; Davis and Capecchi, 1994; Davis et al., 1995; Yokouchi et al., 1995b; Fromental-Ramain et al., 1996; Zakany and Duboule, 1996). Thus, spatiotemporally coordinated expression of *Hox* genes in the limb bud is crucial for pattern formation of limb cartilage elements.

We reported that *Hoxa-11* expression began in the myogenic precursor cells migrating in the limb bud and that *Hoxa-13* was expressed in the posterior region of the muscle, suggesting that *Hox* genes are also involved in muscle patterning (Yamamoto et al., 1998). We also showed that such unique expression patterns of *Hox* genes in the limb muscles are under the control of the limb mesenchyme. However, the actual mesenchymal molecules responsible for inducing *Hox* gene expression in the limb muscles and differences in the effects on the muscle precursor cells and mesenchymal cells have not been determined yet. Thus, we analyzed the effects of the signaling molecules on the HOXA-11 and HOXA-13 expression in the limb muscle precursor cells. Our results indicated that FGF-like activity was involved in the initiation of HOXA-11 expression in the muscle precursor cells and HGF/SF was required for maintenance of the expression. BMP-2 induced the expression of HOXA-13 only in the muscle masses and this was crucial for following subsequent muscle pattern formation. These results suggest that there are differences in the mechanisms of regulation of *Hox* gene expression in the mesenchyme and muscle precursor cells of the chick limb bud.

MATERIALS AND METHODS

Chick surgery

All experimental manipulations were performed in White Leghorn chick embryos. Eggs were incubated at 38°C and the embryos were staged according to Hamburger and Hamilton (1951). The AER removal was performed as described previously (Laufer et al., 1994). At stages 19-21, the AER was removed with a sharpened tungsten needle. Then the embryos were then allowed to develop for 12, 24 or 48 hours or 8 days. Removal of the polarizing region was performed as described previously (Pagan et al., 1996). The polarizing region was excised with a tungsten needle at stages 19-21 and the embryos were allowed to develop for 48 hours or 8 days.

Grafting of beads to the flank or the anterior margin of chick wing buds

Bead implantation was performed as described previously (Brand-Saberi et al., 1996a). Heparin-acrylic beads (H5263, Sigma) were soaked in one of the following; 500 μg/ml recombinant human bFGF(FGF-2) (R and D systems), 400 μg/ml recombinant human HGF/SF (R and D systems), or 5-600 μg/ml *Xenopus* BMP-2 (a gift from Dr Naoto Ueno of the National Institute for Basic Biology) for 1-2 hours at room temperature. Beads soaked in FGF-2 or HGF/SF were placed into a slit in the lateral plate mesoderm of stage 13-19 chick embryos and these embryos were harvested 12, 24 or 48 hours after grafting. Beads soaked in HGF/SF or BMP-2 were grafted to the anterior margin of stage 19-23 chick wing buds. These embryos were harvested 24, 36 or 48 hours or 8 days after grafting.

Grafting of beads to the AER removed limb bud

The AER was dissected from the wing bud at stage 19/20 as described above. Then, the beads soaked in FGF-2 (500 μg/ml) or HGF/SF (400 μg/ml) were implanted into the limb bud immediately or 12 hours after AER removal.

Cell implantation

Transfection of COS7 cells was performed as described by Koshida et al. (1998). The plasmids used were pCDM8 (In Vitrogen) containing *Xenopus Noggin*, *Xenopus Chordin* cDNA or *lacZ* (Sasai et al., 1994). Transplantation of COS7 cells was performed as described previously (Yonei et al., 1993). Cells were pelleted by centrifugation and then dissected with a diameter of approximately 100 μm.

Immunohistochemical staining

Immunohistochemical staining was performed as described previously (Yokouchi et al., 1995b; Yamamoto et al., 1998). The embryos were fixed in methanol/DMSO (4:1) overnight. For preparing cryostat sections, the embryos were not fixed. Guinea pig anti-HOXA-11 IgG and rabbit anti-HOXA-13 IgG were prepared as described by Yamamoto et al. (1998) and Yokouchi et al. (1995b), respectively. For immunohistochemical staining of whole embryos, the specimens were treated with the primary antibodies, guinea pig anti-HOXA-11 IgG (1:3000 dilution), rabbit anti-HOXA-13 IgG (1:8000) and mouse anti-PAX-7 IgG (1:1000; Kawakami et al., 1997). They were then washed and treated with the secondary antibodies, HRP-conjugated rabbit anti-guinea pig IgG (Zymed; 1:500), goat anti-rabbit IgG (Zymed; 1:500) and rabbit anti-mouse IgG (Zymed; 1:500), respectively. If necessary, the embryos were cleared in benzyl alcohol:benzylbenzoate (1:2). For HOXA-11 and PAX-7 double staining of sections, the sections were treated with guinea pig anti-HOXA-11 IgG (1:400) and mouse monoclonal anti-PAX-7 IgG (1:400) at 4°C overnight. After several washes with PBS, sections were incubated with FITC-conjugated anti-guinea pig IgG (1:400; Cappel) and rhodamine-conjugated anti-mouse IgG (1:400; Sigma).

Color visualization for 13F4 (Troponin T) or PAX-7 in the sections

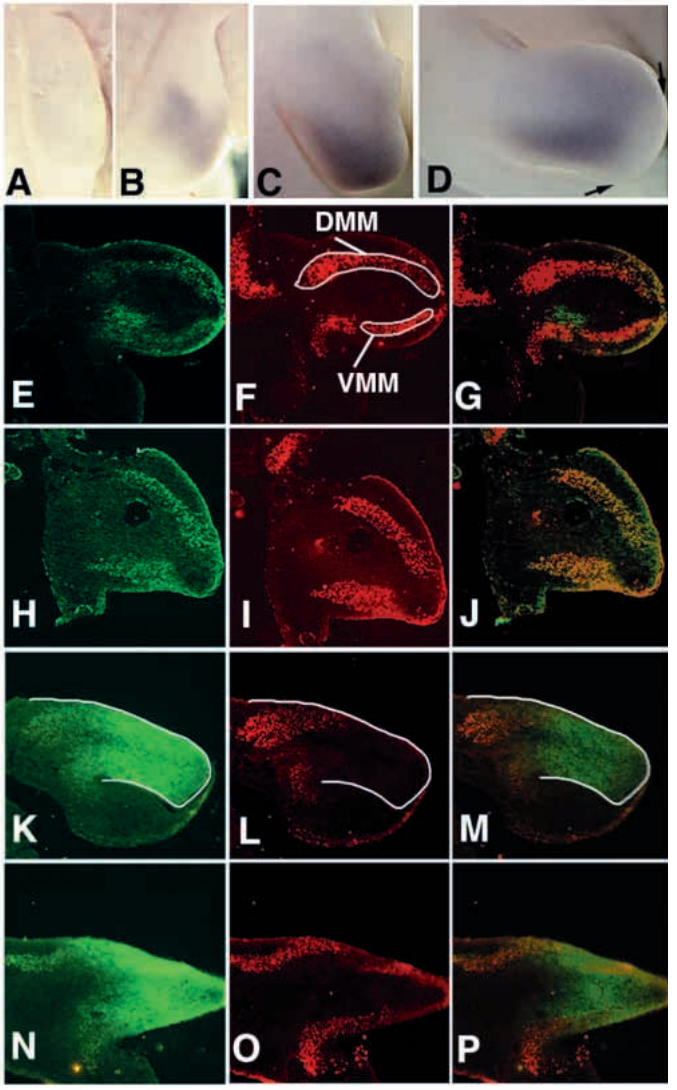

Fig. 1. Effects of AER removal on HOXA-11 expression in the wing bud. Whole-mount detection of HOXA-11 in the AER-removed wing bud at stage 20 followed by incubation for 24 (A) or 48 hours (C), and control wings (B,D). Transverse sections of wing, harvested 24 (E-G) or 48 (K-M) hours after AER removal, and control wings (H-J,N-P). Signals on the sections were as follows: HOXA-11, green (E,H,K,N); PAX-7, red (F,I,L,O); HOXA-11 and PAX-7, orange (merged; G,J,M,P). In the sections, dorsal is to the top and distal is to the right. (A) HOXA-11 expression was lost at stage 23 in the AER-removed wing bud. (B) Contralateral untreated wing bud for comparison. (C) HOXA-11 expression was resumed at stage 25. (D) HOXA-11 expression in the contralateral untreated wing bud. HOXA-11 expression in the myoblasts disappeared completely at stage 23 on sections of AER-removed wing buds (E,G), compared with HOXA-11 expression in H and J. HOXA-11 expression was restored at stage 25 in the myoblasts and mesenchyme (N,P) to the same level as in the contralateral wing (K,M).

was performed with a Vectastain Elite ABC kit (Vector). The cryostat sections were treated with mouse monoclonal anti-Troponin T IgG (13F4; 1:4; DSHB; Rong et al., 1987) or mouse monoclonal anti-PAX-7 IgG (1:400). Then, sections were treated with biotinylated horse anti-mouse IgG (1:200) and incubated for 30 minutes with Vectastain Elite ABC reagent.

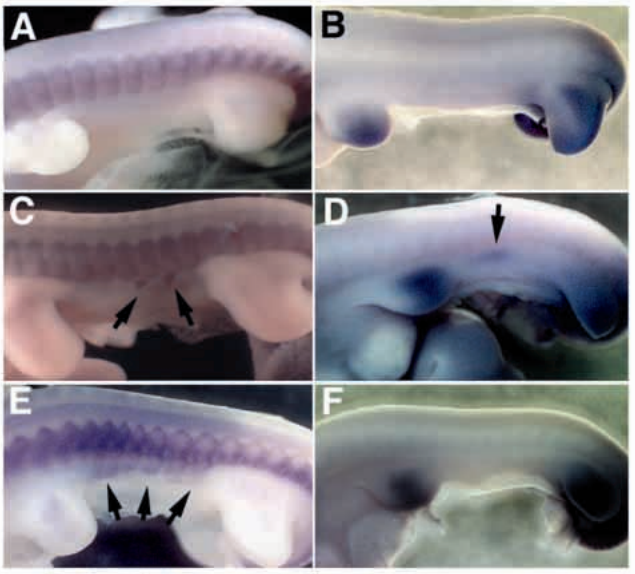

Fig. 2. Effects of FGF-2- or HGF/SF-soaked bead implantation in the flank on HOXA-11 expression. Chicken embryos were subjected to whole-mount immunohistochemistry to detect PAX-7 (A,C,E) and HOXA-11 (B,D,F). (A,B) Embryos that had been implanted with beads soaked in PBS showed the normal patterns of PAX-7 and HOXA-11 expression. (C,D) Embryos were implanted with beads soaked in 500 μg/ml FGF-2. Ectopic migration of PAX-7-positive cells into the interlimb flank at 24 hours after bead implantation, is indicated by arrows (C). Ectopic HOXA-11 expression was observed in the vicinity of ectopic PAX-7-positive cells (D; arrow). (E) Beads soaked in 400 μg/ml HGF/SF usually evoked dispersed delamination of dermamyotomal cells at the lateral edge of somites (arrows). (F) However, no expression of HOXA-11 was seen in the corresponding interlimb region.

RESULTS

Effects of AER removal on HOXA-11 expression

Hoxa-11 expression begins in the prospective zeugopodal mesenchyme at stage 19 (Yokouchi et al., 1991). Detailed immunohistochemical analysis revealed that HOXA-11 was evident in the myogenic precursor cells in the early limb bud outside of the mesenchymal expression domain (Yamamoto et al., 1998). In addition, HOXA-11 expression in the myogenic precursor cells was induced by the limb mesenchyme (Yamamoto et al,. 1998). Together, these results suggested that the regulation of unique HOXA-11 expression in the myogenic precursor cells is different from that in the zeugopodal mesenchyme.

Since HOXA-11 expression in the ectopic migrating myogenic precursor cells at the flank level was induced by implantation of lateral plate mesoderm from the presumptive limb bud region into the flank (Yamamoto et al., 1998), limb mesenchyme is sufficient to induce HOXA-11 expression in the muscle precursor cells. The AER is a prerequisite for cell growth in the progress zone, which produces the initial outgrowth of the limb mesenchyme and is also crucial for expression of some *Hox* genes in the mesenchyme (Hayamizu et al., 1994). Thus, we tested whether HOXA-11 expression in the myogenic precursor cells was dependent on the presence of the AER. During normal limb muscle

development, HOXA-11 expression was first detected in the PAX-7-positive myogenic precursor cells in the limb region at stage 19. The expression began to decrease at stage 24 and disappeared completely by stage 26. AER removal led to abrogation of HOXA-11 expression in the wing buds within 24 hours (earlier stages; 4/4; Fig. 1A), in contrast to the unmanipulated contralateral side (Fig. 1B). However, at 48 hours after AER removal (later stages), HOXA-11 expression was recovered (6/7; Fig. 1C), although the shape of the HOXA-11 re-expression domain was slightly different from that of the normal wing bud. The HOXA-11-free region formed in the distal end of the normal wing bud (Fig. 1D; arrow) was absent in AER-removed wing buds (Fig. 1C). In addition, the region of HOXA-11 expression was smaller than that in the normal counterpart. This might have been because AER-removed wings failed to develop structures located more distally than the proximal zeugopod (Saunders, 1948; Summerbell, 1974; Summerbell and Lewis, 1975; Rowe and Fallon, 1982).

To determine whether the disappearance of HOXA-11 at an earlier stage observed in whole-mount specimens was consistent with ablation of the myogenic precursor cells, we identified these cells in the sections. PAX-7-positive myogenic cells were observed in the AER-removed wing bud, and these separated into the DMM and VMM as in normal development (compare Fig. 1F and I). However, HOXA-11 expression was hardly detected in the myogenic cells in the AER-removed wing buds (4/5; Fig. 1E). No HOXA-11/PAX-7 double-positive cells were observed in the AER-removed wing bud (Fig. 1G; orange). The myogenic tissue extended to within 100 μm of the distal tips of these shortened limb buds (Fig. 1F). These results were in marked contrast to the situation in normal limb buds, in which, depending on the stage, there is always a 200 to 600 μm region containing no myoblasts at the distal tip (Newman et al., 1981; Fig. 1I). This would have been due to cell death in the subridge mesoderm caused by AER removal (Janners and Searls, 1971; Summerbell, 1977; Rowe et al., 1982).

To examine HOXA-11 expression at a later stage, we detected HOXA-11-expressing cells in sections of the AER-removed limb buds (Fig. 1K-M). HOXA-11 expression in both PAX-7-positive myogenic cells and mesenchyme was detected as in normal development (4/4; compare Fig. 1K-M and N-P).

These observations revealed that HOXA-11 expression in both the myogenic cells and mesenchyme at earlier stages is under the control of the AER, but is not at later stages.

HOXA-11 expression in emigrating myoblasts is induced by FGF

HOXA-11 expression in the myoblasts was transiently downregulated by AER removal. As the AER is a source of FGF signal (Niswander et al., 1993; Laufer et al., 1994; Xu et al., 1998) and mesenchymal FGF-10 expression is dependent on the AER (Ohuchi et al., 1997), it is possible that FGF-like signals activate the expression of HOXA-11 in the myoblasts of the limb bud. To examine this possibility, beads soaked in FGF-2 at 500 μg/ml were implanted into the flank of the interlimb region at stage 13-19. Myogenic precursor cells were detached from somites at the level of the implanted bead (visualized by anti-PAX-7 antibody, Fig. 2C arrows). Ectopic HOXA-11 was detected in the region of ectopic migrating myogenic precursor cells (6/6; Fig. 2D; arrows). Beads soaked in PBS did not release ectopic PAX-7-positive cells from somites of the interlimb region and never induced ectopic HOXA-11 expression (4/4, Fig. 2A,B). To determine whether the ectopic HOXA-11-expressing cells corresponded to ectopic myogenic cells, cryosections were double-stained with anti-HOXA-11 antibody and anti-PAX-7 antibody. The HOXA-11 signal in the interlimb region corresponded to the ectopic PAX-7-positive cells (3/3; Fig. 3F; orange). Control beads did not induce delamination of migrating myogenic precursor cells from the dermamyotomal epithelium and did not induce ectopic HOXA-11 expression (3/3, Fig. 3A-C). These results suggested that the FGF-like signals from the limb mesenchyme induce HOXA-11 in the myoblasts of the limb bud.

HGF/SF maintained HOXA-11 expression in the myoblasts

The implantation of FGF beads in the lateral plate mesoderm rapidly induced HGF/SF expression and HGF/SF induced delamination of the cells from the dermamyotome (Heymann et al., 1996; Brand-Saberi et al., 1996a). Thus, FGF might induce HOXA-11 expression in the myoblasts through induction of HGF/SF. To determine the involvement of HGF/SF in induction of HOXA-11 expression, beads loaded with HGF/SF at 400 μg/ml were implanted into the flank at stage 15. Migration of the myogenic precursor cells into the lateral plate mesoderm was observed (4/4; Fig. 2E; arrows), however no expression of HOXA-11 was observed in the delaminated cells (13/13; Fig. 2F). To determine whether weak HOXA-11 expression was missed in whole-mount specimens, we examined HOXA-11 expression on sections. However, no HOXA-11 expression was detected in the ectopic migrating myogenic precursor cells (7/7; Fig. 3G-I; arrows).

As described above, ectopic HGF/SF cannot induce HOXA-11 expression in the ectopic myogenic precursor cells. We postulated that HGF/SF is required for the maintenance of HOXA-11 expression in the myogenic precursor cells, because the disappearance of HOXA-11 expression in the myogenic precursor cells occurs concomitantly with disappearance of HGF/SF in the limb mesenchyme during normal development. To examine this possibility, HGF/SF beads were implanted into the anterior margin of the wing buds at stage 23, the stage at which HOXA-11 expression begins to decrease slightly during normal development. (Fig. 3O-Q). Continuous HOXA-11 expression was observed in the myoblasts adjacent to the HGF/SF beads 36 hours after implantation at which time HOXA-11 in the myoblasts disappeared during normal development (Fig. 3K-M; arrowheads). At the same time, the number of myoblasts increased by 1.37±0.02-fold (mean ± s.e.m.) in the HGF/SF-bead-treated wings as compared to controls (Fig. 3L compared with Fig. 3P). However, the muscle pattern was not altered at stage 35 (data not shown).

These results demonstrated that HGF/SF could not induce HOXA-11 expression in the myoblasts in the limb bud but maintained HOXA-11 expression.

Regulation of HOXA-11 expression by FGF and HGF/SF

To obtain more information on the effect of FGF and HGF/SF

on HOXA-11 expression in the myogenic cells and mesenchyme, we next analyzed the effects of these signals in AER-removed wing buds by implantation of FGF-2 or HGF/SF beads.

We implanted FGF-2 beads into stage 20 wing buds immediately after AER removal, or at 12 hours after AER removal, at which time point HOXA-11 expression had disappeared completely. These embryos were allowed to develop until stage 23. HOXA-11 expression was downregulated in the AER-removed wing buds implanted with PBS beads similarly to AER-removed wings at early stages (5/7; Fig. 4A,B). On the contrary, HOXA-11 expression was activated around the FGF-2 beads in the wings implanted at immediately after AER removal (7/7; Fig. 4C). HOXA-11 was re-expressed in the wing buds implanted with FGF-2 beads even after HOXA-11 had disappeared following AER removal (3/3; Fig. 4D). In addition, in the sections of wings implanted with FGF-2 beads both 0 and 12 hours after AER removal, we detected HOXA-11 protein in both the PAX-7-positive myogenic cells and mesenchyme (Fig. 5A-C), although cells in the immediate vicinity of FGF-2 beads were devoid of HOXA-11. These results showed that FGF signals could maintain/activate HOXA-11 in the myogenic cells and mesenchyme.

Implantation of HGF/SF beads promptly after AER removal maintained HOXA-11 expression in the myogenic cells (5/5; Fig. 4E). On sections of the AER-removed wings implanted with HGF/SF beads, we detected HOXA-11 expression in the PAX-7-positive myogenic cells, but not in the mesenchymal cells (Fig. 5D-F). Implantation of HGF/SF beads 12 hours after AER removal, in contrast, induced little or no re-expression of HOXA-11 (3/5; Fig. 4F). On cryostat sections of these specimens, HOXA-11 expression was not observed in either the myogenic precursor cells or the mesenchyme (2/2; Fig. 5G-I). These observations indicate that HGF/SF plays a role in the maintenance of HOXA-11 expression only in the myoblasts of the limb bud and not in the limb mesenchyme.

HOXA-13 in the posterior region of muscle masses was induced by signal(s) from the polarizing region

HOXA-13 expression was first observed in the posterior regions of both DMM and VMM and in the prospective autopodal mesenchyme (Fig. 6B,D; Yamamoto et al., 1998). At later stages, HOXA-13 expression in the musculature showed a dynamic pattern correlated with the splitting process of the muscle masses (Yamamoto et al., 1998).

To examine the signal(s) required for HOXA-13 expression in the posterior regions of the muscle masses, we analyzed HOXA-13 expression in the AER-removed wings. HOXA-13 expression in the distal mesenchyme disappeared 36 hours after AER removal (Fig. 6A compared with B). On the contrary, HOXA-13 in the myoblasts of the posterior muscle masses was retained at the same levels as in the controls (Fig. 6A,B). Following removal of the polarizing region from the wing buds, HOXA-13 expression in the distal mesenchyme exhibited no changes. However, HOXA-13 in the myoblasts of the posterior muscle masses disappeared completely or was severely reduced (3/6; Fig. 6C).

To address whether posterior regions of the muscle masses had been eliminated physically during removal of the polarizing region or were left intact, we examined PAX-7 expression on cryostat sections (Fig. 6F,H). In the wings from which the polarizing region had been removed, we confirmed the existence of two muscle masses. However, the muscle masses changed their position along the dorsoventral axis (Fig. 6F). In the sections of the wing buds with the polarizing region removed, HOXA-13 signals completely disappeared from the posterior region of the muscle masses (Fig. 6E) compare to the control wing buds (Fig. 6G). These findings suggested that HOXA-13 expression is regulated in a different manner in the myoblasts and mesenchyme, and that the activation of HOXA-13 in the myoblasts of the posterior muscle masses is dependent on the polarizing signal(s), but not on the AER.

Following removal of the polarizing region, the cartilage patterns along the anteroposterior and proximodistal axes were severely altered. No cartilage elements other than the humerus and radius were observed in the most severe phenotype. Muscle patterning also collapsed, which may have been due to a deficiency of splitting both along the anteroposterior and dorsoventral axes (Fig. 6I-M). Whereas the extent of both PAX-7 and Troponin T expression was not changed in wings with the polarizing region removed (Fig. 6I,J).

BMP-2 induced ectopic HOXA-13 expression in the anterior region of the muscle masses

As described above, HOXA-13 expression in the myoblasts of the posterior muscle masses requires signal(s) from the polarizing region. SHH has polarizing activity and induces mesenchymal *Bmp-2* expression in the posterior part of the limb bud (Laufer et al., 1994). We tested the effects of BMP-2 on HOXA-13 expression in the posterior part of muscle masses. Beads soaked in BMP-2 were implanted into the anterior margin of the wing buds at stage 20. We found that ectopic expression of HOXA-13 was induced as a strip in the anterior region of the wing bud using BMP-2 beads at 100 μg/ml (4/6; Fig. 7B; arrowheads) and 50 μg/ml (5/7; Fig. 7C). The beads soaked in 5,300 μg/ml and 600 μg/ml BMP-2 could not activate ectopic HOXA-13 expression in the anterior region of the wing buds (Fig. 7A,D). To verify whether the ectopic expression of HOXA-13 was present in the muscle masses, we examined HOXA-13 expression on cross sections of stage 25 wings implanted with 100 μg/ml BMP-2 beads. Ectopic expression of HOXA-13 was detected in the anterior region of the VMM and the number of HOXA-13-positive cells in the anterior region of the DMM increased significantly (Fig. 7G-I; arrows). In addition, HOXA-13 expression in the posterior region of the muscle masses extended into more anterior regions. We observed no ectopic HOXA-13 expression in control embryos implanted with beads soaked in PBS (11/11; Fig. 7E). These results indicated that BMP-2 activates *Hoxa-13* in the posterior region of the muscle masses.

The effect of application of exogenous BMP-2 on limb cartilage development was dependent on the concentration. At 300 or 600 μg/ml, the radius and ulna in the zeugopod were shortened and thickened and the ectopic digit was induced anterior to digit 2 (6/9; Fig. 7J). No tendons or muscles were observed in the ectopic digits (data not shown). At 50 or 100 μg/ml, ectopic expression of HOXA-13 was induced in the anterior region of the muscle masses, and radius and ulna were shortened but digits were unaffected (data not shown; 5/6). At 5 μg/ml, no effects were observed (data not shown; 11/11). The cartilage phenotypes induced by 300 or 600 μg/ml were similar

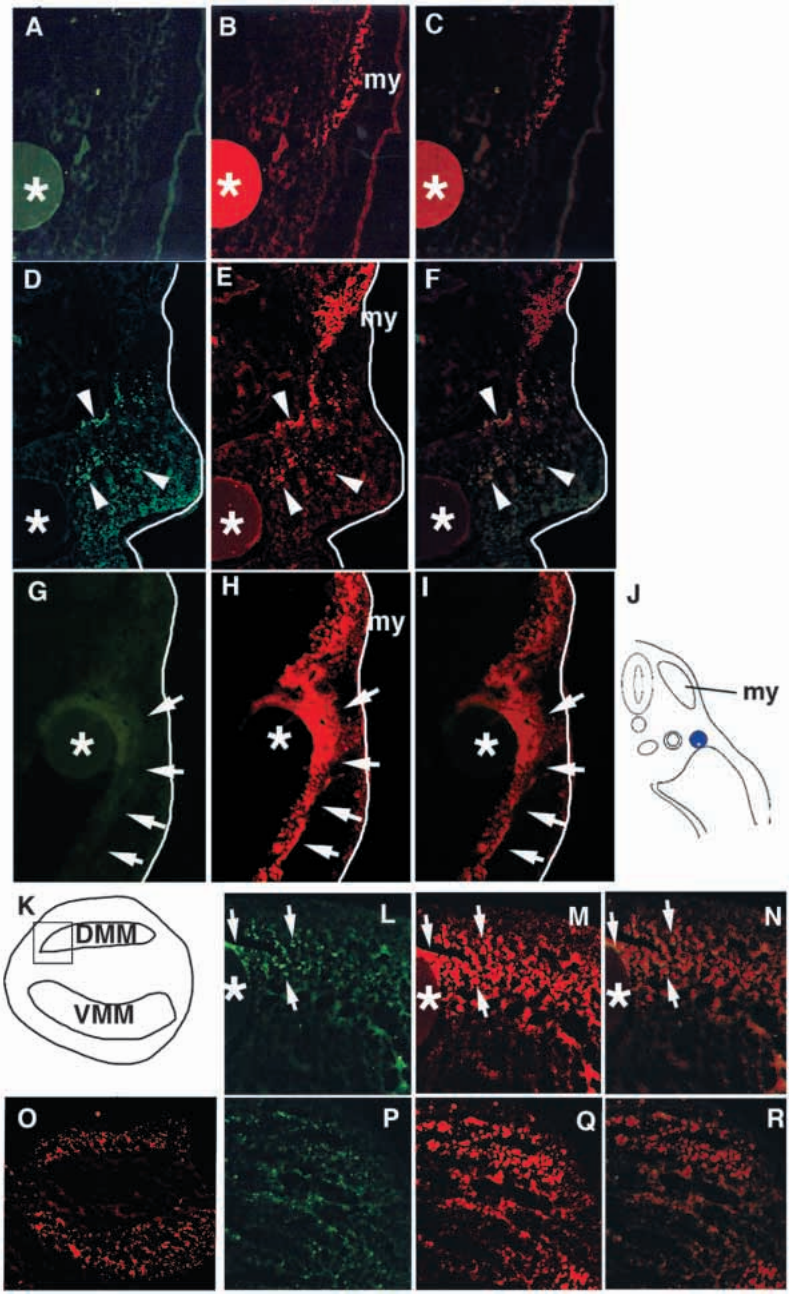

Fig. 3. FGF induces HOXA-11 expression in ectopic myogenic precursor cells and HGF/SF maintains the expression in the myogenic precursor cells in the limb bud. (J) The figure shows the region of sections A-I. The cross sections were subjected to immunohistochemical staining for HOXA-11 (A,D,G; green), PAX-7 (B,E,H; red), HOXA-11 and PAX-7 (C,F,I; merged: orange). Specimens implanted with PBS-soaked beads (A-C), FGF-2 (500 μg/ml)-soaked beads (D-F), HGF (400 μg/ml)-soaked beads (G-I). The application of FGF-2 (500 μg/ml)-soaked bead into interlimb region induced migration of PAX-7-positive myogenic precursor cells into the lateral plate mesoderm 12 hours after implantation (E). HOXA-11 expression was detected in these ectopic myogenic precursor cells (D,F; arrowheads). The application of HGF/SF induced delamination of dermamyotomal cells (H; arrows). However, HOXA-11 expression was not observed in ectopic PAX-7-positive cells of the interlimb region (G,I; arrows). Note that beads soaked in PBS did not induce delamination of dermamyotomal cells or ectopic HOXA-11 expression (A-C). Asterisks show positions of beads. (B,E,H,J) my; dermamyotome. (A-J) Dorsal is to the top and lateral is to the right. (K-R) Dorsal is to the top and anterior is to the left. Cross sections of stage 26 wing buds implanted with beads soaked in 400 μg/ml of HGF/SF at the anterior margin; (L) HOXA-11, (M) PAX-7, (N) HOXA-11 and PAX-7 (merged), and contralateral wing bud (P, HOXA-11; O and Q, PAX-7; R, HOXA-11 and PAX-7 (merged)). (O) Cross section of control wing stained with anti-PAX-7 antibody. (K) Schematic drawing of the muscle pattern. Box indicates the position corresponding to P-R. In the control wing, HOXA-11 expression in PAX-7-positive cells had already been lost (P,R). In contrast, in the HGF bead-implanted wings, HOXA-11 expression was detected near the bead (L,N; arrows). In addition, the number of PAX-7-positive cells was increased near the beads (M) as compared with the control (Q). DMM, dorsal muscle mass; VMM, ventral muscle mass.

to the pattern reported previously using implantation of BMP-2-expressing cells into the limb bud (Duprez et al., 1996).

The effect of BMP-2 application on the limb muscle development was dependent on the concentration. In the wings implanted with beads soaked in 300 or 600 μg/ml BMP-2, the radius was thickened and the muscles in the vicinity of the radius were smaller and distorted in shape due to the enlarged cartilage, but the muscle pattern did not change (Fig. 7J). In contrast, when 50 or 100 μg/ml BMP-2 beads were implanted, ectopic muscles were induced near the beads (Fig. 7M; arrowheads). Embryos implanted with 50 or 100 μg/ml BMP-2 beads had no ectopic digits or tendons, and thus the ectopic muscle was induced autonomously. At 5μg/ml, there were no differences in muscle development between implanted and control wings.

HOXA-13 expression in the muscle masses was repressed by NOGGIN/CHORDIN application

As described above, ectopic BMP-2 induced ectopic HOXA-13 expression in the muscle masses. We then examined the effect of interruption of intrinsic BMP-2 signaling by transplantation of cells producing the BMP-2 antagonists, NOGGIN and CHORDIN (Sasai et al., 1994; Piccolo et al., 1996; Zimmerman et al., 1996). Following grafting of *Noggin/Chordin*-transfected COS7 cells into the posterior margin, stripe-like HOXA-13 expression was significantly downregulated (Fig. 8B), but *lacZ*-transfected COS7 cells had no effect (Fig. 8A). This change in HOXA-13 expression was confirmed to be in the muscle masses by analysis of sections (Fig. 8E-H). However, HOXA-13 expression in the autopodal mesenchyme was not changed in wings implanted with

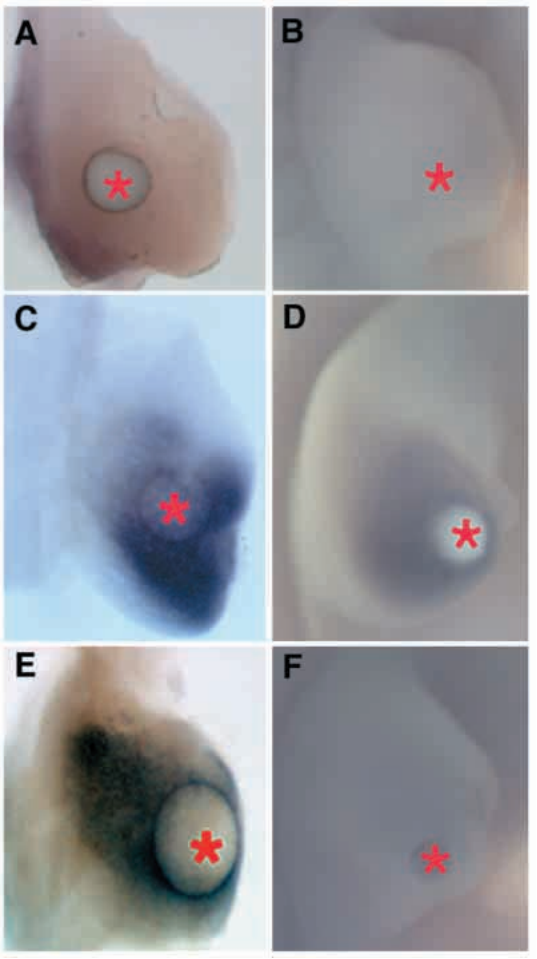

Fig. 4. HOXA-11 expression in the AER-removed wing was restored by application of FGF or HGF/SF. At stage 20, AER was removed, and beads were implanted immediately (A,C,E) or 12 hours (B,D,E) after AER removal. (C,D) beads soaked in 500 μg/ml FGF-2; (E,F) 400 μg/ml HGF/SF; (A,B) PBS as control. The embryos were harvested at 24 hours (A,C,E) and 12 hours after beads implantation (B,D,E). Wing buds implanted with FGF-2-soaked beads immediately after AER removal, HOXA-11 was detected after 24 hours incubation (C). HOXA-11 was also detected after 12 hours incubation in wing buds implanted with FGF-2-soaked beads 12 hours after AER-removal (D). Implantation of 400 μg/ml HGF/SF-soaked beads immediately after AER removal maintained HOXA-11 expression after 24 hours incubation (E). However, implantation of HGF/SF-soaked beads 12 hours after AER removal did not induce HOXA-11 expression (F). Note that beads soaked in PBS did not maintain or induce HOXA-11 in the wing bud (A,B).

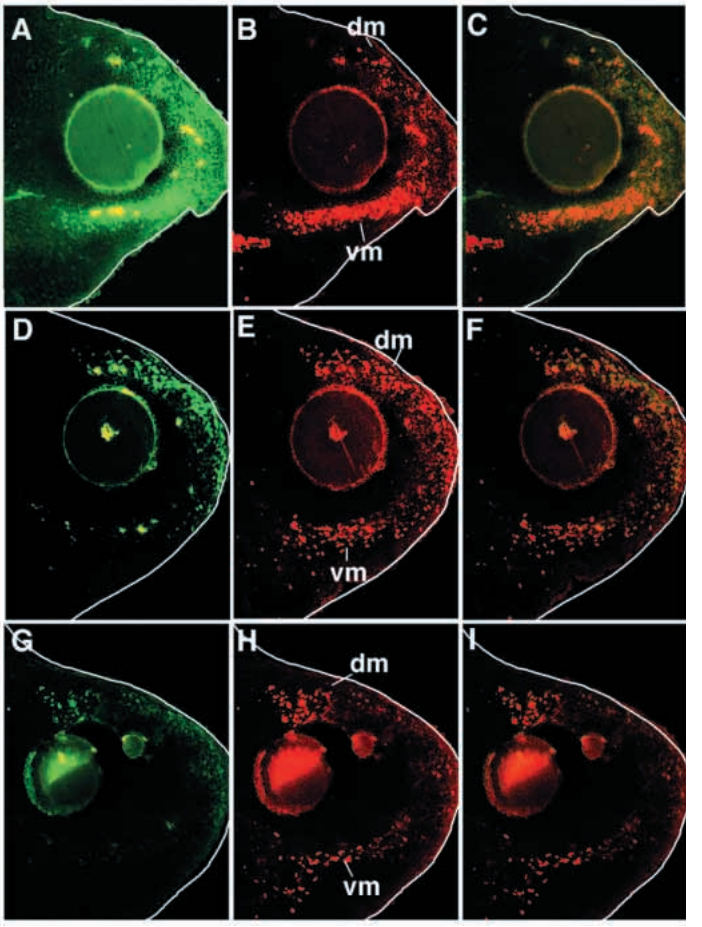

Fig. 5. Distribution of the cells re-expressing HOXA-11 in the AER-removed limb buds implanted FGF-2- or HGF/SF-soaked beads. (A-C) Sections of the limb buds implanted with FGF-2-soaked beads at 12 hours after AER removal. (D-F) Sections of wing buds implanted with HGF/SF-soaked beads at immediately after AER removal. (G-I) Sections of wing buds implanted with HGF/SF-soaked beads at 12 hours after AER removal. The sections were stained for HOXA-11 (A,D,G; green) and PAX-7 (B,E,H; red). HOXA-11/PAX-7 (C,F,I; orange; merged). HOXA-11 expression was seen in the PAX-7-positive myogenic cells and mesenchymal cells in FGF-2-implanted wings (A-C). Note that the mesenchymal cells adjacent to the beads never showed HOXA-11 expression, and most of HOXA-11-positive mesenchymal cells were located distally to the bead. Immediate implantation of HGF/SF-soaked beads maintained HOXA-11 expression in PAX-7-positive myogenic cells, but not in the mesenchymal cells (D-F). HOXA-11 expression was observed in the myogenic cells adjacent to the beads. The expression of HOXA-11 was hardly detected in the wing buds implanted with HGF/SF-soaked beads at 12 hours after AER removal (G-I).

Noggin/Chordin- or *lacZ*-transfected COS7 cells (Fig. 8A,B). Implantation of *Noggin/Chordin*-transfected COS7 cells into the autopod induced no significant changes in HOXA-13 expression in either the muscle masses or in the autopodal mesenchyme (Fig. 8C). We therefore concluded that interruption of intrinsic BMP signaling in the limb bud inhibited muscle-specific HOXA-13 expression.

Grafting of *Noggin/Chordin*-transfected COS7 cells into the posterior margin of the wing bud also led to a change in cartilage shape. The ulna was shortened and sometimes digit **3** disappeared (Fig. 8D). The typical feature of the wings implanted with *Noggin/Chordin*-transfected COS7 cells are shown in Fig. 8I and J. The muscle pattern was distorted, the number of myogenic cells was decreased (Fig. 8I) and the quantity of Troponin T, a marker of muscle differentiation, was markedly reduced (Fig. 8J) in the PAX-7-positive cells as compared with controls (Fig. 8K,L). However, the number of PAX-7-positive cells or Troponin T expression was not affected by removal of the polarizing region (Fig. 6I,J) and ectopic BMP-2 application (data not shown).

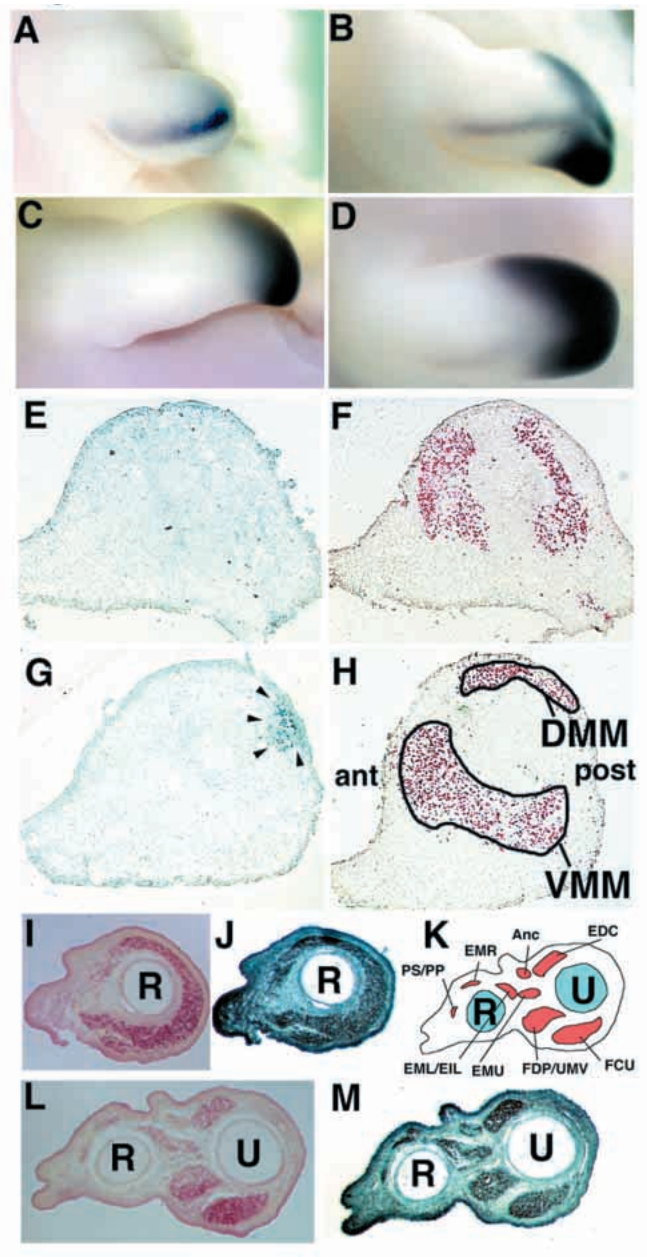

Fig. 6. Effects of removal of the AER or the polarizing region on HOXA-13 expression. Distribution of HOXA-13 proteins in stage 20 (A) AER-removed wing and (B) contralateral wing. (A) HOXA-13 in the mesenchyme was lost leaving muscular expression. Distribution of HOXA-13 proteins in stage 20 polarizing region-removed wing (C) and contralateral wing (D). (C) HOXA-13 in the posterior region of the muscle masses disappeared. However, its expression in the mesenchyme was not changed. Neighboring cross sections of stage 25 wings with the polarizing region removed (E,F) and contralateral wing (G,H) stained for HOXA-13 (E,G) and PAX-7 (F,H). HOXA-13 expression in the posterior region of the muscle mass had completely disappeared in the polarizing region-removed wing (E) compared with the contralateral wing (G; arrowheads). In the manipulated wing, muscle masses were not located precisely along dorsoventral axis (F). Neighboring cross-sections of the wing with polarizing region removed harvested at stage 30 (I,J) and of the contralateral wing were stained for PAX-7 (I,L) and Troponin T (J,M). In the wing with (L,M) the polarizing region removed, the ulna disappeared and the muscle masses were no longer separated into the dorsal and ventral regions (4/6; I,J). The removal of the polarizing region, however, did not suppress splitting of the muscle masses completely. Note that the quantity of Troponin T was comparable to the normal amount in the PAX-7-positive cells in the wing with polarizing region removed. (K) Schematic view of the muscle pattern in L,M. Muscle identification and muscle nomenclature are according to Shellswell and Wolpert (1977), Robson et al. (1994) and Murray and Wilson (1997). R, radius; U, ulna; DMM, dorsal muscle mass; VMM, ventral muscle mass; PS/PP, pronator superficials/pronator profundus; EMR, extensor metacarpi radialis; Anc, anconeus; EDC, extensor digitorum communis; EML/EIL, extensor medius longus/extensor indicis longus; EMU, extensor metacarpi ulnaris; FDP/UMV, flexor digitorum profundus/ulnimetacarpalis ventralis; FCU, flexor carpi ulnaris.

In addition, we observed abnormalities in angiogenesis in implanted wings. Forced expression of constitutively active *BMPR-IA* in the limb bud induced ectopic vascularization in the limb cartilage elements (Zou et al., 1997). These results indicated that BMP signaling plays a role in angiogenesis in the embryo.

DISCUSSION

Many studies have demonstrated that the spatially and temporally coordinated expression of *Hox* genes in the limb mesenchyme is crucial for limb cartilage pattern formation. In this study, we analyzed the signaling molecules that control coordinated expression of *Hoxa-11* and *Hoxa-13* during limb muscle development. Our findings indicated that FGF, HGF/SF and BMP-2 signaling differentially control *Hoxa-11* and *Hoxa-13* expression in the limb muscle precursor cells and limb mesenchymal cells.

FGF signal is involved in the induction of HOXA-11 expression in the muscle precursor and mesenchymal cells

HOXA-11 expression was specifically detected in the myogenic precursor cells of the limb bud, but not in the interlimb region. Transplantation of the presumptive limb bud region into the interlimb region induced ectopic migration of the myogenic precursor cells out the somites at the flank level (Hayashi and Ozawa, 1995). Ectopic expression of HOXA-11 was observed in the ectopic migrating myogenic precursor cells (Yamamoto et al., 1998). Thus, the signals from the limb mesenchyme were supposed to induce HOXA-11 expression in the muscle precursor cells when they invaded the limb bud. Likewise, FGF bead implantation into the flank induced ectopic limb bud development and at the same time that ectopic muscle precursor migration was induced (Cohn et al., 1995; Fig. 3D-F). We showed that FGF application also induced ectopic HOXA-11 expression in the ectopic muscle precursor cells of the flank (Figs 2D, 3D-F). FGF-4 and FGF-8, which can induce limb bud formation, are expressed in the AER and act on the outgrowth of the limb bud (for review, see Martin, 1998). FGF-2 and FGF-10, which are expressed in the limb mesenchyme, both induce limb bud formation and migration of the myogenic precursor cells (for review, see Martin, 1998). Thus, one or more of these FGFs in the limb bud may induce HOXA-11 expression in the myogenic precursor cells.

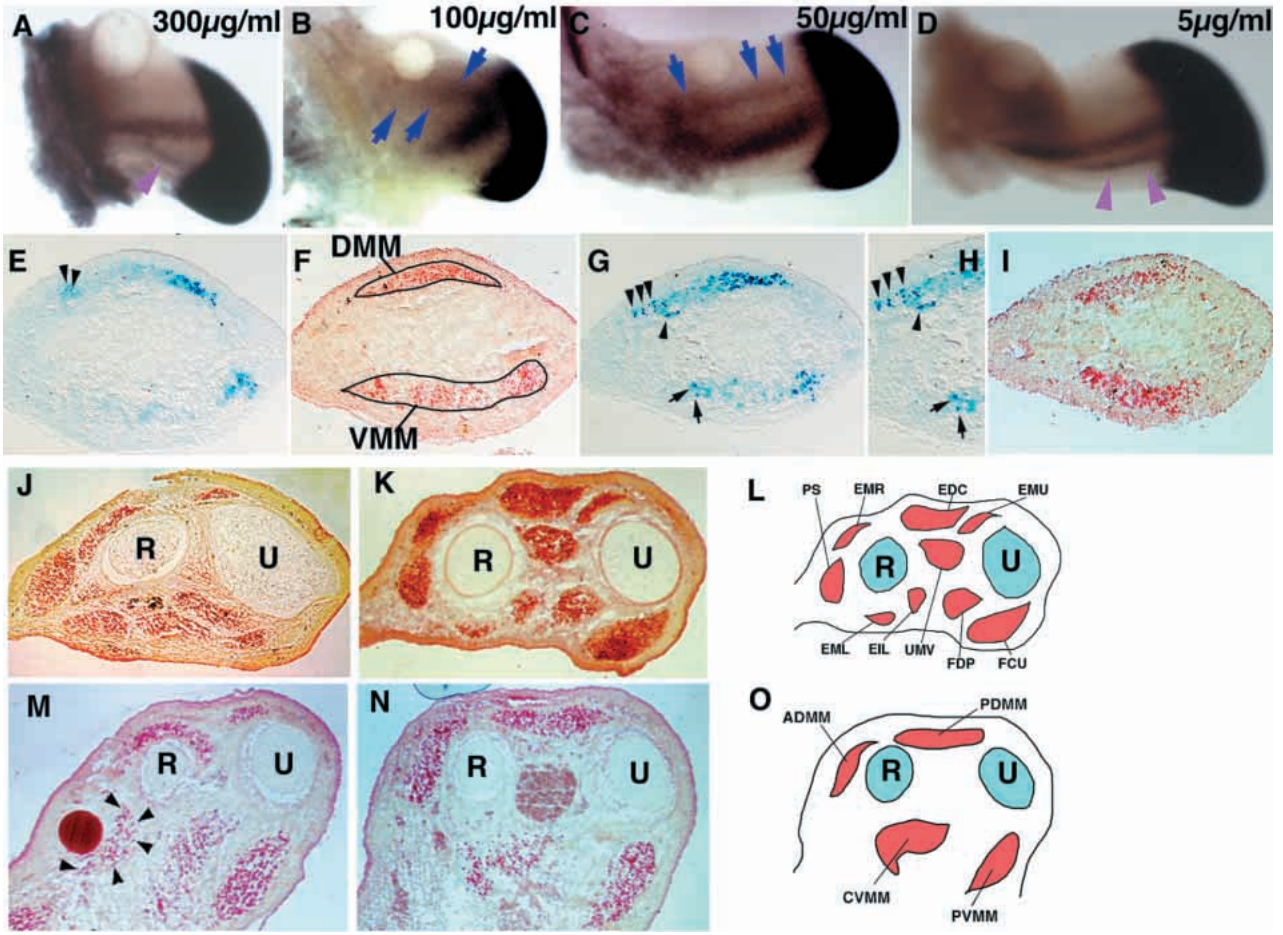

Fig. 7. BMP signaling activates HOXA-13 expression in the muscle masses. Beads soaked with BMP-2 at various concentration were implanted into the stage 19/20 wing buds and harvested 48 hours after implantation. (A) Dorsal view of the wing following implantation of 300 μg/ml BMP-2-soaked beads into the anterior margin. There was no significant differences in HOXA-13 expression between wings implanted with 300 μg/ml BMP-2-soaked beads and controls. (A-D) Because the embryos were cleared, HOXA-13 expression in both DMM and VMM are visible depending on the angle of view. Pink arrowheads in A and D indicate HOXA-13 expression in the posterior region of the VMM. (B) Dorsal view of the wing following implantation of 100 μg/ml BMP-2-soaked beads into the anterior margin. This led to ectopic HOXA-13 expression in the anterior region of the limb bud (blue arrows). (C) Dorsal view of the wing following implantation of 50 μg/ml BMP-2-soaked beads into the anterior margin. Ectopic HOXA-13 expression in the anterior region was observed. Application of 50-100 μg/ml BMP-2-soaked beads resulted in expansion of the region of HOXA-13 expression (B,C compared with A,D). (D) Dorsal view of the wing following implantation of 5 μg/ml BMP-2-soaked beads into the anterior margin. No ectopic HOXA-13 expression was induced in the anterior region. Neighboring sections of stage 25 wings following implantation of 50 μg/ml BMP-2-soaked beads into the anterior margin (G,I) and those of the wings implanted with beads soaked in PBS (E,F), stained for HOXA-13 (E,G) and PAX-7 (F,I). (H) Higher magnification of the anterior region in G. Following application of BMP-2 into the anterior margin, HOXA-13 expression in the posterior muscle masses spread anteriorly (G compared with E), the number of HOXA-13-expressing cells increased at the most anterior region of the DMM (E,G,H; arrowheads) and ectopic HOXA-13 expression was induced at the most anterior region of the VMM (G,H; arrows). (J-O) The effect of BMP-2 implantation on muscle pattern formation. (J) Cross-section of the wing implanted with 600 μg/ml BMP-2-soaked bead, and (K) the contralateral untreated wing at stage 34. (M) Cross-section of the wing implanted with 50 μ g/ml BMP-2-soaked bead, and (N) the contralateral untreated wing at stage 28. (L) Schematic view of the muscle pattern in K. (O) Schematic view of the muscle pattern in control wing (N). Following implantation of beads soaked in 50 μg/ml BMP-2, ectopic muscle was formed in the anterior mesenchyme close to the beads (M; the area surrounded by arrowheads; 3/8). In the ectopic PAX-7-positive myogenic cells, the amount of Troponin T was unaffected normally (data not shown). R, radius; U, ulna; ADMM, anterior dorsal muscle mass; PDMM, posterior dorsal muscle mass; CVMM, central ventral muscle masses; PVMM, posterior ventral muscle mass. Muscle identification and nomenclature in L as in Fig. 6. (E-O) In the sections, dorsal is to the top and anterior is to the left.

HGF/SF is expressed in the limb mesenchyme (Myokai et al., 1995; Brand-Saberi et al., 1996a; Heymann et al., 1996). Application of FGF-2 beads induced ectopic HGF/SF expression in the mesenchyme (Brand-Saberi et al., 1996a). HGF/SF bead implantation induced delamination of the dermamyotomal cells (Figs 2E, 3H; Brand-Saberi et al., 1996a; Heymann et al., 1996); however, no HOXA-11 expression was observed in the ectopic myogenic precursor cells (Figs 2F, 3H,I). These results indicated that HOXA-11 expression in the myogenic precursor cells of the limb bud was induced by FGF signaling or unknown factor(s) induced by FGF but not via HGF/SF. Previous studies have shown that *lbx1*, a vertebrate

homologue of the *Drosophila ladybird* gene, is expressed in the limb muscle precursor cells (Jagla et al., 1995). In the muscle precursor cells, *lbx1* begins to be expressed a little earlier than HOXA-11. *Lbx1* as well as HOXA-11 are activated by ectopic FGF, but not activated by HGF/SF bead in the flank (Mennerich et al., 1998) suggesting that they are regulated by the same mechanism.

Two phases for the maintenance of HOXA-11 expression in the limb muscle precursor cells and mesenchymal cells

At stages 18-23 (earlier stages), HOXA-11 was evident in the myogenic precursor cells. However, expression was not yet observed in the mesenchymal cells. In later stages (at stages 24 and 25), the number of myogenic precursor cells expressing HOXA-11 decreased gradually, while the number of mesenchymal HOXA-11-expressing cells increased (Yamamoto et al., 1998). We showed that HOXA-11 in both the myogenic precursor and mesenchymal cells disappeared by following AER removal at stage 20 (Fig. 1A,E-G), followed by re-expression in both the myogenic and mesenchymal cells at later stages (Fig. 1C,K-M). We never observed regeneration of AER-like structures or FGF-8 re-expression during this experimental period. There are several possible regulatory mechanisms for HOXA-11 re-expression in the myogenic cells and mesenchymal cells. Ohuchi et al. (1997) demonstrated that *fgf10* expression gradually decreased from stage 22 and the expression was dependent on the AER. We showed that ectopic FGF re-activated HOXA-11 expression after FGF-8 (AER) and FGF-10 (mesenchyme) had been eliminated by AER removal (Figs 4C,D, 5A-C). One possibility is that AER removal itself or the signaling system dependent on the AER acts as a trigger for ectopic expression or hyperactivation of molecules with similar functions to FGFs in the remaining ectoderm or in the mesenchyme. Alternatively, myogenic cells may undergo autonomous activation. Maintenance of *Hox* expression in the limb muscle at earlier phases may require FGF signaling from the AER and, after establishment of the autocrine loop by FGF-like signaling in the muscle masses, *Hox* expression may become dependent on this circuit. For instance, FGF-1 and FGF-2 proteins in proliferating skeletal muscle cells act as autocrine regulators of skeletal muscle development in vitro

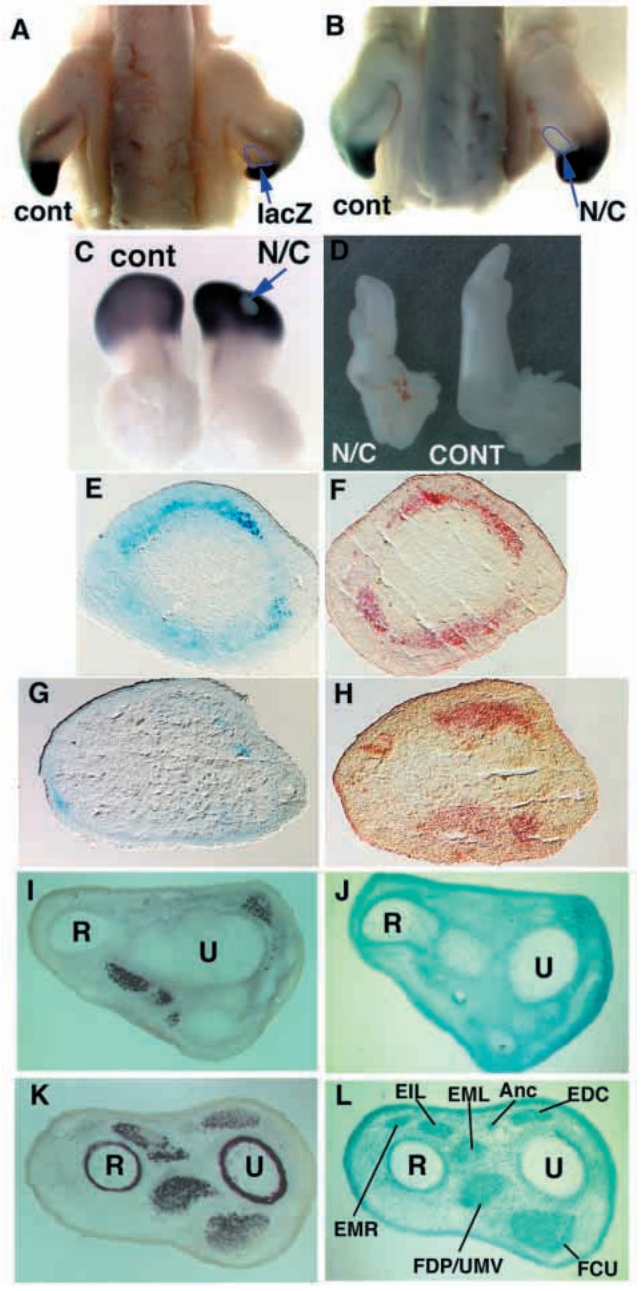

Fig. 8. Implantation of *Noggin/Chordin*-transfected COS7 cells into the posterior region of the limb bud inhibited intrinsic HOXA-13 expression in the posterior region of the muscle masses. (A) The posterior mesenchyme of the right wing was implanted with *Noggin/Chordin*-transfected COS7 cells into at stage 19/20 and harvested at stage 25. HOXA-13 expression in the posterior region of the muscle masses showed a marked decrease compared to the contralateral left wing. (C) Right is the ventral view of the experimental wing with *Noggin/Chordin*-transfected COS7 cells implanted into the distal mesenchyme. The expression of HOXA-13 in both muscle masses and mesenchyme agreed with those in the left contralateral wing. Note that the wing with *lacZ*-transfected COS7 cells implanted into the posterior mesenchyme showed no alteration of the expression pattern of HOXA-13 (B). Juxtaposition of sections of stage 25 wing with *Noggin/Chordin*-transfected COS7 cells implanted into the posterior mesenchyme (G,H) and that of the wing implanted with *lacZ*-transfected COS7 cells (E,F), stained for HOXA-13 (E,G) and PAX-7 (F,H). (E) Following introduction of exogenous NOGGIN/CHORDIN in the posterior mesenchyme, HOXA-13 was hardly detected expression in the posterior region of the muscle masses. At stage 25, there were no differences in PAX-7 expression between the wing to which NOGGIN/CHORDIN was applied and the control wing (F,H). (I-L) The effect of *Noggin/Chordin*-transfected COS7 cells implantation on muscle pattern formation. (D) Left is the wing implanted with *Noggin/Chordin*-transfected COS7 cells and right is the contralateral wing at stage 33. (I,J) Neighboring cross sections of left manipulated wing in D; (K,L) neighboring cross sections of right control wing in D. Distribution of PAX-7 (I,K) and Troponin T (J,L) determined by immunohistochemical staining of the sections. (D) The zeugopodal cartilage were severely shortened. The muscles were reduced and distorted by *Noggin/Chordin*-transfected COS7 cell implantation (I compared with K). In addition, the area of Troponin T-positive region was markedly reduced (J compared with L). R, radius; U, ulna. (E-L) In the sections, dorsal is to the top and anterior is to the left. Muscle identification and nomenclature in L as in Fig. 6.

(Hannon et al., 1996). Similar FGF autocrine mechanisms may be involved in limb muscle development to maintain HOXA-11 expression in the muscle precursor cells. In this case, earlier HOXA-11 maintenance would be under the control of FGF signaling from the AER. At later stages, when the AER is separated from the muscle masses due to limb outgrowth, the autocrine-loop may become prominent for HOXA-11 maintenance.

HOXA-11 expression was not yet initiated in the mesenchyme at stage 19/20 when AER was removed. Thus, HOXA-11 expression in the mesenchyme seemed to be independent of stage 19/20 AER function, while mesenchymal HOXA-11 expression was detected at later stages (Fig. 1C,K-M). As AER removal at stage 19/20 allowed development of a part of the zeugopodal cartilage (Summerbell and Lewis, 1975) and HOXA-11 is expressed in the presumptive zeugopodal mesenchyme, it is possible that HOXA-11 expression is already committed in the cells at stage 19/20 in the progress zone.

HGF/SF maintains HOXA-11 in the muscle precursor cells at earlier phase

In the embryos supplied with FGF-2 or HGF/SF immediately after AER removal, HOXA-11 expression in the muscle precursor cells did not disappear (Figs 4C,E, 5D-F). Those embryos that received exogenous FGF signal at 12 hours after AER removal also showed no loss of HOXA-11 expression (Figs 4D, 5A-C). However, application of HGF/SF 12 hours after AER removal could not restore HOXA-11 expression (Figs 4F, 5G-H). Mesenchymal HGF expression is dependent on FGF signaling from the AER (our unpublished results). Because HGF expression was hyperinduced by FGF bead implantation after AER removal (our unpublished results), this HGF activity would preserve HOXA-11 expression. In contrast, once HOXA-11 expression had disappeared from the muscle precursor cells, HGF was not sufficient to reinitiate HOXA-11 expression. The expression pattern of HGF/SF showed dynamic changes during limb development (Myokai et al., 1995; Brand-Saberi et al., 1996a; Heymann et al., 1996). HGF/SF expression began at stage 17 in the mesenchymal cells of the entire limb bud. At stage 22, it began to decrease in the proximodistal direction and became restricted to the mesenchyme of the distal tip. This spatiotemporal expression profile of HGF/SF was similar to that of HOXA-11 expression in the limb muscle cells. Implantation of HGF into the limb bud suppressed the decrease in HOXA-11 expression in the myogenic precursor cells (Fig. 3L-N). Our results suggested that HGF/SF, which was induced by FGF, is required for maintenance of the earlier phase HOXA-11 expression in the muscle masses.

BMP-2 is required for HOXA-13 expression in the posterior region of the muscle masses

The polarizing region controls not only cartilage pattern but also muscle pattern along the anteroposterior axis (Robson et al., 1994). SHH, which is a primary signal from the polarizing region, increases the proliferation rate of the myoblasts (Duprez et al., 1998) and induces *Bmp-2* in the posterior mesenchyme (Laufer et al., 1994). Administration of BMP-2 into the anterior margin of the limb bud induced ectopic HOXA-13 expression in the anterior region of the muscle masses (Fig. 7B,C,G,H). On the contrary, application of *Noggin/Chordin*-transfected COS7 cells into the posterior region of the limb bud abolished intrinsic HOXA-13 expression in the posterior region of the muscle masses (Fig. 8B,E,F). Thus, expression of HOXA-13 in the posterior region was dependent on the BMP-2 signaling. Application of ectopic BMP-2 was shown to activate ectopic *Hoxd-13* expression in the anterior mesenchyme (Duprez et al., 1996), although its biological significance is still unclear. In contrast, BMP-2 was not involved in the regulation of HOXA-13 expression in the mesenchyme (Fig. 7A-I). This would be due to differences in sensitivity to BMP signaling between *Hox* clusters.

AER removal downregulated *Bmp-2* expression in the posterior mesenchyme of the limb bud (Laufer et al., 1994). However, our results showed that muscular HOXA-13, supposed to be dependent on BMP-2, was not downregulated by AER removal (Fig. 6A). This apparent conflict could be explained as follows. *Bmp-2* expression was first detected at stage 16/17 in the posterior mesenchyme (Francis et al., 1994) and BMP-2 signaling may have activated secondary signals in the limb mesenchyme that were more widespread than the *Bmp-2* expression domain resulting in activation of HOXA-13 expression in the myoblasts. Alternatively, BMP-2 may induce HOXA-13 expression directly in the muscle masses. In this case, *Hoxa-13* expression in the posterior myogenic precursor cells had already been committed by BMP-2 at stage 19/20, when AER was removed. Once committed, *Hoxa-13* started to be expressed independently of further BMP-2 signaling. A definitive answer must await elucidation of the signals downstream of BMP-2, and interruption of BMP-2 signaling specific for muscle precursor cells, e.g. by forced expression of dominant-negative BMPR in the muscle precursor cells.

Function of BMP signaling via HOXA-13 in the muscle masses in muscle development

Administration of BMP-2 into the anterior margin of the limb bud induced ectopic HOXA-13 expression in the anterior region of the muscle masses (Fig. 7B,C,G,H), followed by ectopic muscle formation in the anterior region (Fig. 7M). Unfortunately application of *Noggin/Chordin*-transfected COS7 cells to mimic loss-of-function mutation distorted cartilage and muscle pattern too severely to determine the effects of BMP-2 signaling on muscle patterning and did not help elucidate the function of posterior HOXA-13 in muscle patterning.

Therefore, we will base our discussion on the results of the gain-of-function experiment. Since administration of BMP-2 at some concentrations amplified the myogenic precursor population (Amthor et al., 1998), application of BMP-2 beads would stimulate proliferation of the muscle precursor cells in the anterior limb bud. This could explain the production of ectopic muscle and in this case, induction of ectopic HOXA-13 is independent from the ectopic muscle formation. However, stimulation of proliferation of the muscle precursors by uniform expression of *shh* in the limb bud neither changes the muscle pattern nor facilitates muscle mass splitting (Duprez et al., 1998). In this case, local changes in the proliferation rates of the muscle precursor cells, controlled by positional signaling, may be crucial for muscle patterning. It is still possible that HOXA-13 is involved in controlling proliferation

as a downstream component of the BMP signaling cascade. Alternatively, ectopic muscle may have been formed by ectopically induced splitting of the muscle mass by ectopic HOXA-13 in the anterior region of the muscle masses. The muscle precursor cells expressing HOXA-13 may have different cell-cell interactions from non-expressing cells. The molecular mechanisms of the muscle splitting process are not yet known. Cell-cell adhesion molecules may be involved in this process. Adhesion molecules such as N-cadherin are expressed in the limb muscle (Brand-Saberi et al., 1996b). *Hox* genes were demonstrated to be involved in the mesenchymal cell-cell adhesion process (Yokouchi et al., 1995b; Newman, 1996; Packer et al., 1997) and, specifically, *Hox* genes can directly regulate N-CAM transcription (Edelman and Johns, 1995). Eph receptors and ligands, which mediate repulsive cell-cell interaction, are also expressed in a region-specific manner in the limb muscle masses (personal communication from Dr H. Tanaka, Kumamoto University). *Hox* genes directly regulate expression of the *Eph* gene in the hindbrain (Chen and Ruley, 1998). Thus, it is likely that HOXA-13 in the posterior muscle masses is involved in controlling these cell-cell interacting molecules followed by muscle splitting.

Different effects of signaling molecules on *Hoxa-11* and *Hoxa-13* expression in the muscle precursors and mesenchyme of the limb bud

In this study, we showed that coordinated expression of HOXA-11 and HOXA-13 in the limb muscle is regulated by signals from neighboring limb mesenchymal cells. HOXA-11 expression in the muscle precursor cells is initiated by FGF signal(s) and maintained by HGF/SF signal from the limb mesenchyme. HOXA-11 expression in the mesenchyme is induced by FGF signal(s), but is not affected by the HGF/SF signal. On the contrary, HGF has no effect on HOXA-13 expression in either the mesenchymal or muscle precursor cells (results not shown). HOXA-13 expression in the posterior muscle masses is induced by the polarizing signal via BMP-2. In contrast, HOXA-13 expression in the autopodal mesenchyme is independent of the polarizing region but is dependent on the signals from the AER.

In addition to the limb bud, rhombomere-specific expression of *Hox* genes in the hindbrain requires signals from the interacting mesoderm tissue (Gould et al., 1998). In addition, the same *Hox* genes are expressed in the different tissues, exhibiting crucial functions in each tissue (Dolle et al., 1993; Yokouchi et al., 1995a; Kondo et al., 1996). *Hox* genes seem to have *cis* regulatory elements responsible for the tissue-specific induction/maintenance signals for production of spatially coordinated expression without changing temporal colinearity.

We are grateful to Dr Y. Sasai for providing *Xenopus Chordin* and *Noggin* cDNAs, Dr N. Ueno for the gift of *Xenopus* BMP-2 and Dr A. Kawakami for the gift of mouse anti-PAX-7 monoclonal IgG. This work was supported in part by 'The Mitsubishi Foundation', by a Grant-in-aid of Ministry of Education, Science and Culture, Japan, and by CREST (Core Research for Evolutional Science and Technology) of Japan Science and Technology Corporation (JST).

REFERENCES

Amthor, H., Christ, B., Weil, M. and Patel, K. (1998). The importance of timing differentiation during limb muscle development. *Curr. Biol.* **8**, 642-652.

Birchmeier, C. and Gherardi, E. (1998). Developmental roles of HGF/SF and its receptor, the c-Met tyrosine kinase. *Trends Cell Biol.* **8**, 404-410.

Brand-Saberi, B., Muller, T. S., Wilting, J., Christ, B. and Birchmeier, C. (1996a). Scatter factor/hepatocyte growth factor (SF/HGF) induces emigration of myogenic cells at interlimb level *in vivo*. *Dev. Biol.* **179**, 303-308.

Brand-Saberi, B., Gamel, A. J., Krenn, V., Muller, T. S., Wilting, J. and Christ, B. (1996b). N-cadherin is involved in myoblast migration and muscle differentiation in the avian limb bud. *Dev. Biol.* **178**, 160-173.

Chen, J. and Ruley, H. E. (1998). An enhancer element in the *EphA2 (Eck)* gene sufficient for rhombomere- specific expression is activated by HOXA1 and HOXB1 homeobox proteins. *J. Biol. Chem.* **273**, 24670-24675.

Chevallier, A., Kieny, M. and Mauger, A. (1977). Limb-somite relationship: origin of the limb musculature. *J. Embryol. Exp. Morph.* **41**, 245-258.

Cohn, M. J., Izpisua-Belmonte, J. C., Abud, H., Heath, J. K. and Tickle, C. (1995). Fibroblast growth factors induce additional limb development from the flank of chick embryos. *Cell* **80**, 739-746.

Daston, G., Lamar, E., Olivier, M. and Goulding, M. (1996). *Pax-3* is necessary for migration but not differentiation of limb muscle precursors in the mouse. *Development* **122**, 1017-1027.

Davis, A. P. and Capecchi, M. R. (1994). Axial homeosis and appendicular skeleton defects in mice with a targeted disruption of *hoxd-11*. *Development* **120**, 2187-2198.

Davis, A. P., Witte, D. P., Hsieh-Li, H. M., Potter, S. S. and Capecchi, M. R. (1995). Absence of radius and ulna in mice lacking *hoxa-11* and *hoxd-11*. *Nature* **375**, 791-795.

Dolle, P., Izpisua-Belmonte, J. C., Falkenstein, H., Renucci, A. and Duboule, D. (1989). Coordinate expression of the murine *Hox-5* complex homoeobox-containing genes during limb pattern formation. *Nature* **342**, 767-772.

Dolle, P., Dierich, A., LeMeur, M., Schimmang, T., Schuhbaur, B., Chambon, P. and Duboule, D. (1993). Disruption of the *Hoxd-13* gene induces localized heterochrony leading to mice with neotenic limbs. *Cell* **75**, 431-441.

Duprez, D. M., Kostakopoulou, K., Francis-West, P. H., Tickle, C. and Brickell, P. M. (1996). Activation of Fgf-4 and HoxD gene expression by BMP-2 expressing cells in the developing chick limb. *Development* **122**, 1821-1828.

Duprez, D., Fournier-Thibault, C. and Le Douarin, N. (1998). *Sonic Hedgehog* induces proliferation of committed skeletal muscle cells in the chick limb. *Development* **125**, 495-505.

Edelman, G. M. and Jones, F. S. (1995). Developmental control of N-CAM expression by *Hox* and *Pax* gene products. *Phil. Trans R. Soc. Lond. B Biol. Sci.* **349**, 305-312.

Francis, P. H., Richardson, M. K., Brickell, P. M. and Tickle, C. (1994). Bone morphogenetic proteins and a signaling pathway that controls patterning in the developing chick limb. *Development* **120**, 209-218.

Fromental-Ramain, C., Warot, X., Messadec, N., LeMeur, M. P. D. and Chambon, P. (1996). Hoxa-13 and Hoxd-13 play a crucial role in the patterning of the limb autopod. *Development* **122**, 2997-3011.

Gould, A., Itasaki, N. and Krumlauf, R. (1998). Initiation of rhombomeric *Hoxb4* expression requires induction by somites and a retinoid pathway. *Neuron* **21**, 39-51.

Hamburger, V. and Hamilton, H. L. (1951). A series of normal stages in the development of the chick embryo. *J. Morph.* **94**, 257-265.

Hannon, K., Kudla, A. J., McAvoy, M. J., Clase, K. L. and Olwin, B. B. (1996). Differentially expressed fibroblast growth factors regulate skeletal muscle development through autocrine and paracrine mechanisms. *J. Cell Biol.* **132**, 1151-1159.

Hayamizu, T. F., Wanek, N., Taylor, G., Trevino, C., Shi, C., Anderson, R., Gardiner, D. M., Muneoka, K. and Bryant, S. V. (1994). Regeneration of *HoxD* expression domains during pattern regulation in chick wing buds. *Dev. Biol.* **161**, 504-512.

Hayashi, K. and Ozawa, E. (1995). Myogenic cell migration from somites is induced by tissue contact with medial region of the presumptive limb mesoderm in chick embryos. *Development* **121**, 661-669.

Heymann, S., Koudrova, M., Arnold, H., Koster, M. and Braun, T. (1996). Regulation and function of SF/HGF during migration of limb muscle precursor cells in chicken. *Dev. Biol.* **180**, 566-578.

Izpisua-Belmonte, J. C., Tickle, C., Dolle, P., Wolpert, L. and Duboule, D. (1991). Expression of the homeobox Hox-4 genes and the specification of position in chick wing development. *Nature* **350**, 585-589.

Jagla, K., Dolle, P., Mattei, M. G., Jagla, T., Schuhbaur, B., Dretzen, G., Bellard, F. and Bellard, M. (1995). Mouse *Lbx1* and human *LBX1* define a novel mammalian homeobox gene family related to the *Drosophila lady bird* genes. *Mech. Dev.* **53**, 345-356.

Janners, M. Y. and Searls, R. L. (1971). Effect of removal of the apical ectodermal ridge on the rate of cell division in the subridge mesenchyme of the embryonic chick wing. *Dev. Biol.* **24**, 465-476.

Kawakami, A., Kimura-Kawakami, M., Nomura, T. and Fujisawa, H. (1997). Distributions of PAX6 and PAX7 proteins suggest their involvement in both early and late phases of chick brain development. *Mech. Dev.* **66**, 119-130.

Kondo, T., Dolle, P., Zakany, J. and Duboule, D. (1996). Function of posterior HoxD genes in the morphogenesis of the anal sphincter. *Development* **122**, 2651-2659.

Koshida, S., Shinya, M., Mizuno, T., Kuroiwa, A. and Takeda, H. (1998). Initial anteroposterior pattern of the zebrafish central nervous system is determined by differential competence of the epiblast. *Development* **125**, 1957-1966.

Laufer, E., Nelson, C. E., Johnson, R. L., Morgan, B. A. and Tabin, C. (1994). *Sonic hedgehog* and Fgf-4 act through a signaling cascade and feedback loop to integrate growth and patterning of the developing limb bud. *Cell* **79**, 993-1003.

Martin, G. R. (1998). The roles of FGFs in the early development of vertebrate limbs. *Genes Dev.* **12**, 1571-1586.

Mennerich, D., Schafer, K. and Braun, T. (1998). *Pax-3* is necessary but not sufficient for *lbx1* expression in myogenic precursor cells of the limb. *Mech. Dev.* **73**, 147-158.

Morgan, B. A., Izpisua-Belmonte, J. C., Duboule, D. and Tabin, C. J. (1992). Targeted misexpression of *Hox-4.6* in the avian limb bud causes apparent homeotic transformations. *Nature* **358**, 236-239.

Murray, B. and Wilson, D. J. (1997). Muscle patterning, differentiation and vascularisation in the chick wing bud. *J. Anat.* **190**, 261-273.

Myokai, F., Washio, N., Asahara, Y., Yamaai, T., Tanda, N., Ishikawa, T., Aoki, S., Kurihara, H., Murayama, Y., Saito, T. et al. (1995). Expression of the *hepatocyte growth factor* gene during chick limb development. *Dev. Dyn.* **202**, 80-90.

Newman, A. S., Pautou, P., M. and Kieny, M. (1981). The distal boundary of myogenic primodia in chimeric avian limb buds and its relation to an accessible population of cartilage progenitor cells. *Dev. Biol.* **84**, 440-448.

Newman, S. A. (1996). Sticky fingers: *Hox* genes and cell adhesion in vertebrate limb development. *BioEssays* **18**, 171-174.

Niswander, L., Tickle, C., Vogel, A., Booth, I. and Martin, G. R. (1993). FGF-4 replaces the apical ectodermal ridge and directs outgrowth and patterning of the limb. *Cell* **75**, 579-587.

Nohno, T., Noji, S., Koyama, E., Ohyama, K., Myokai, F., Kuroiwa, A., Saito, T. and Taniguchi, S. (1991). Involvement of the *Chox-4* chicken homeobox genes in determination of anteroposterior axial polarity during limb development. *Cell* **64**, 1197-1205.

Ohuchi, H., Nakagawa, T., Yamamoto, A., Araga, A., Ohata, T., Ishimaru, Y., Yoshioka, H., Kuwana, T., Nohno, T., Yamasaki, M. et al. (1997). The mesenchymal factor, FGF10, initiates and maintains the outgrowth of the chick limb bud through interaction with FGF8, an apical ectodermal factor. *Development* **124**, 2235-2244.

Olson, E. N. and Klein, W. H. (1994). BHLH factors in muscle development: dead lines and commitments, what to leave in and what to leave out. *Genes Dev.* **8**, 1-8.

Packer, A. I., Elwell, V. A., Parnass, J. D., Knudsen, K. A. and Wolgemuth, D. J. (1997). N-cadherin protein distribution in normal embryos and in embryos carrying mutations in the homeobox gene *Hoxa-4*. *Int. J. Dev. Biol.* **41**, 459-468.

Pagan, S. M., Ros, M. A., Tabin, C. and Fallon, J. F. (1996). Surgical removal of limb bud. *Sonic hedgehog* results in posterior skeletal defects. *Dev. Biol.* **180**, 35-40.

Parr, B. A. and McMahon, A. P. (1995). Dorsalizing signal *Wnt-7a* required for normal polarity of D-V and A-P axes of mouse limb. *Nature* **374**, 350-353.

Piccolo, S., Sasai, Y., Lu, B. and De Robertis, E. M. (1996). Dorsoventral patterning in *Xenopus*: inhibition of ventral signals by direct binding of chordin to BMP-4. *Cell* **86**, 589-598.

Riddle, R. D., Ensini, M., Nelson, C., Tsuchida, T., Jessell, T. M. and Tabin, C. (1995). Induction of the LIM homeobox gene Lmx1 by WNT7a establishes dorsoventral pattern in the vertebrate limb. *Cell* **83**, 631-640.

Robson, L. G., Kara, T., Crawley, A. and Tickle, C. (1994). Tissue and cellular patterning of the musculature in chick wings. *Development* **120**, 1265-1276.

Rong, P. M., Ziller, C., Pena-Melian, A. and Le Douarin, N. M. (1987). A monoclonal antibody specific for avian early myogenic cells and differentiated muscle. *Dev. Biol.* **122**, 338-353.

Rowe, D. A., Cairns, J. M. and Fallon, J. F. (1982). Spatial and temporal patterns of cell death in limb bud mesoderm after apical ectodermal ridge removal. *Dev. Biol.* **93**, 83-91.

Rowe, D. A. and Fallon, J. F. (1982). The proximodistal determination of skeletal parts in the developing chick leg. *J. Embryol. Exp. Morph.* **68**, 1-7.

Sasai, Y., Lu, B., Steinbeisser, H., Geissert, D., Gont, L. K. and De Robertis, E. M. (1994). *Xenopus* chordin: a novel dorsalizing factor activated by organizer- specific homeobox genes. *Cell* **79**, 779-90.

Saunders J.W., J. (1948). The proximal-distal sequence of origin of the parts of the chick wing and the role of ectoderm. *J. Exp. Zool.* **108**, 363-404.

Schramm, C. and Solursh, M. (1990). The formation of premuscle masses during chick wing bud development. *Anat. Embryol.* **182**, 235-247.

Shellswell, G. B. and Wolpert, L. (1977). The pattern of muscle and tendon development in the chick wing. In *Vertebrate Limb and Somite Morphogenesis* (ed. D. A. Ede, J. R. Hinchliffe and M. Balls) Cambridge: Cambridge University Press.

Small, K. M. and Potter, S. S. (1993). Homeotic transformations and limb defects in *Hox A11* mutant mice. *Genes Dev.* **7**, 2318-2328.

Summerbell, D. (1974). A quantitative analysis of the effect of excision of the AER from the chick limb-bud. *J. Embryol. Exp. Morph.* **32**, 651-660.

Summerbell, D. and Lewis, J. H. (1975). Time, place and positional value in the chick limb-bud. *J. Embryol. Exp. Morph.* **33**, 621-643.

Summerbell, D. (1977). Reduction of the rate of outgrowth, cell density, and cell division following removal of the apical ectodermal ridge of the chick limb bud. *J. Embryol. Exp. Morph.* **40**, 1-12.

Vogel, A., Rodriguez, C., Warnken, W. and Izpisua-Belmonte, J. C. (1995). Dorsal cell fate specified by chick *Lmx1* during vertebrate limb. *Nature* **378**, 716-720.

Xu, X., Weinstein, M., Li, C., Naski, M., Cohen, R. I., Ornitz, D. M., Leder, P. and Deng, C. (1998). Fibroblast growth factor receptor 2 (FGFR2)-mediated reciprocal regulation loop between FGF8 and FGF10 is essential for limb induction. *Development* **125**, 753-765.

Yamamoto, M., Gotoh, Y., Tamura, K., Tanaka, M., Kawakami, A., Ide, H. and Kuroiwa, A. (1998). Coordinated expression of *Hoxa-11* and *Hoxa-13* during limb muscle patterning. *Development* **125**, 1325-1235.

Yang, X. M., Vogan, K., Gros, P. and Park, M. (1996). Expression of the met receptor tyrosine kinase in muscle progenitor cells in somites and limbs is absent in Splotch mice. *Development* **122**, 2163-2171.

Yokouchi, Y., Sasaki, H. and Kuroiwa, A. (1991). Homeobox gene expression correlated with the bifurcation process of limb cartilage development. *Nature* **353**, 443-445.

Yokouchi, Y., Nakazato, S., Yamamoto, M., Goto, Y., Kameda, T., Iba, H. and Kuroiwa, A. (1995a). Misexpression of *Hoxa-13* induces cartilage homeotic transformation and changes cell adhesiveness in chick limb buds. *Genes Dev.* **9**, 2509-2522.

Yokouchi, Y., Sakiyama, J. and Kuroiwa, A. (1995b). Coordinated expression of *Abd-B* subfamily genes of the *HoxA* cluster in the developing digestive tract of chick embryo. *Dev. Biol.* **169**, 76-89.

Yonei, S., Tamura, K., Koyama, E., Nohno, T., Noji, S. and Ide, H. (1993). MRC-5, human embryonic lung fibroblasts, induce the duplication of the developing chick limb bud. *Dev. Biol.* **160**, 246-253.

Zakany, J. and Duboule, D. (1996). Synpolydactyly in mice with a targeted deficiency in the HoxD complex. *Nature* **384**, 69-71.

Zimmerman, L. B., De Jesus-Escobar, J. M. and Harland, R. M. (1996). The Spemann organizer signal Noggin binds and inactivates Bone morphogenetic protein 4. *Cell* **86**, 599-606.

Zou, H., Wieser, R., Massague, J. and Niswander, L. (1997). Distinct roles of type I bone morphogenetic protein receptors in the formation and differentiation of cartilage. *Genes Dev.* **11**, 2191-2203.